PNAS
www.pnas.org

Supplementary Information for

Nur77 controls tolerance induction, terminal differentiation, and effector functions in semi-invariant natural killer T cells

Amrendra Kumar[1,2], Timothy M. Hill[2,3], Laura E. Gordy[2], Naveenchandra Suryadevara[2], Lan Wu[2], Andrew I. Flyak[2,4], Jelena S. Bezbradica[2,5], Luc Van Kaer[2], and Sebastian Joyce[1,2,6]

Corresponding author: Sebastian Joyce
Email: sebastian.joyce@vumc.org

This PDF file includes:

www.pnas.org/cgi/doi/10.1073/pnas.2001665117

MATERIALS & METHODS

Antibodies and Reagents

All monoclonal antibodies (mAbs) used for the identification of iNKT cells and iNKT cell developmental stages are listed in **Supplementary Table 1** and described before [1, 2]. αGalCer (KRN7000) was purchased from Funakoshi (Japan). CaspGLOW fluorescein Active Caspase-3 (FITC-DEVD-FMK) staining kit, EdU, and Click-iT™ Plus EdU Alexa Fluor™ 488 were from Invitrogen. PE, APC, or BV421 fluorophore-tagged, mouse CD1d-αGalCer tetramers were obtained from the NIH Tetramer Facility (Emory University).

Generation of BM chimeras

Recipient Jα18$^{-/-}$ mice were irradiated with a single dose of 950 rads from a cesium source and rested for 6—8 hours. B6, Nur77^{tg}, Jα18$^{-/-}$, Nur77^{tg};Vα14^{tg} and Vα14^{tg} mice BM cells (10x10^6) were used as donors for transfer into irradiated Jα18$^{-/-}$ recipients alone (single BM chimeras) or mixed at 1:1 ratio with BM cells from Jα18$^{-/-}$ mice (mixed BM chimeras). In some studies, 10x10^6 BM cells from CD45.1$^+$ B6, CD45.2$^+$ Vα14^{tg} or CD45.2$^+$ Nur77^{tg};Vα14^{tg} mice were transferred into irradiated Jα18$^{-/-}$ recipients either alone or mixed in 1:1 ratio with 10x10^6 BM cells from CD45.1$^+$ B6 mice to generate mixed BM chimeras. For limiting dilution studies, 1x10^6, 5x10^6 or 10x10^6 Jα18$^{-/-}$ BM cells were mixed with 10x10^6 Vα14^{tg} or Nur77^{tg};Vα14^{tg} BM cells.

Flow Cytometry

Cells (3x10^6) from indicated mice were incubated with Ghost Violet 510 viability dye to differentiate between live/dead cells. Cells were washed twice with FACS buffer and incubated with FACS buffer containing 0.2 μg anti-CD16/CD32 mAb (Fc receptor blocking Ab) followed by surface staining with CD1d tetramer and antibodies against mouse CD3ε, CD24, CD44 and NK1.1 to evaluate iNKT cell developmental stages and caspase 3 activation by iNKT cells as described previously [1, 2]. Briefly, iNKT cells were identified as CD3ε$^+$tetramer$^+$ cells among B220^{LO}CD8^{LO} splenocytes and hepatic mononuclear cells or B220^{LO}CD8^{LO} thymocytes.

For intracellular detection of cytokines, cells were stained for live dead discrimination and surface stained to identify iNKT cells followed by intracellular staining with mAbs against mouse IFN-γ, IL-4, IL-17 or IL-10 using fixation/permeabilization solution kit (BD Biosciences) by following the manufacturer's protocol. For nuclear staining of transcription factors (TFs), dead cell discrimination and surface staining were done as above followed by nuclear detection of TFs PLZF, Tbet, RORγt, and Foxp3 by using eBiosciences Foxp3/TFs staining buffer set using the manufacturer's protocol. iNKT cell developmental activation profile, stages, subsets were phenotyped by using eight to ten color flow cytometry, which was performed with a FACSCanto II, LSR-II instrument or Fortessa (Becton-Dickinson). Data were analyzed with FlowJo software (Treestar Inc.). Absolute iNKT cell numbers were calculated from % tetramer$^+$ cells and total number of cells recovered from each organ. In some experiments (**Figure 2B; Supplementary Figure 2B**) AccuCheck counting beads (Thermo Fisher Scientific) were included in samples to allow for calculation of absolute iNKT cell counts as per the manufacturer's instructions.

Serum cytokine detection

Animals were injected i.p. with vehicle control or 1 μg αGalCer followed by serum harvest 5—6 hours after injection. Serum cytokines were estimated using Meso Scale Detection multiplex cytokines assay using manufacturer protocols and guidelines.

Antigen presentation assay

DP thymocytes isolated from 5—6-week old Vα14^{tg} and Nur77^{tg};Vα14^{tg} mice were flow sorted. Purified DP thymocytes (5x10^5) were incubated with the test Vα14$^+$ iNKT cell hybridoma (DN32.D3; 5x10^4) or the control Vα3.2$^+$ hybridoma (431-A11; 5x10^4) cells. Supernatants from the co-culture were collected after 24 hours, and IL-2 production was quantified by enzyme-linked immunosorbent assay as described [1].

Apoptosis and cell proliferation assay

For caspase 3 apoptosis assay, thymocytes and splenocytes (3×10^6) from indicated mice were incubated with FITC labelled caspase 3 (FITC-DEVD-FMK) or control (Z-VAD-FMK) substrates for 3 hours. Cells were washed twice (with wash buffer included in CaspGLOW fluorescein active caspase assay kit) and incubated with Ghost Violet 510 viability dye. Cells were washed twice with FACS buffer and incubated with FACS buffer containing 0.2 μg anti-CD16/CD32 mAb followed by surface staining with CD1d tetramer and mAbs against mouse CD3ε, CD24, CD44 and NK1.1 to evaluate caspase 3 activation by total iNKT cells or each developmental stage as described previously [1, 2]. For cell proliferation assay, mice were injected i.p. with 1 mg 5-ethynyl-2- 611 deoxyuridine (EdU) in PBS for 72 hours before analysis. Cells were stained to discriminate live from dead cells, and block Fc receptors. Cells were surface stained to identify iNKT cells and each developmental stage as above. EdU incorporation was detected with Click-iT™ Plus EdU Alexa Fluor™ 488 by following the manufacturer's protocol. EdU incorporation was analyzed in live iNKT cells by flow cytometry.

Statistics

Comparisons between three or more groups were performed by one-way ANOVA with Tukey's post test to determine significance. Comparison between two groups was performed by two-tailed, unpaired *t* test. All statistical analyses were performed using Prism software (GraphPad).

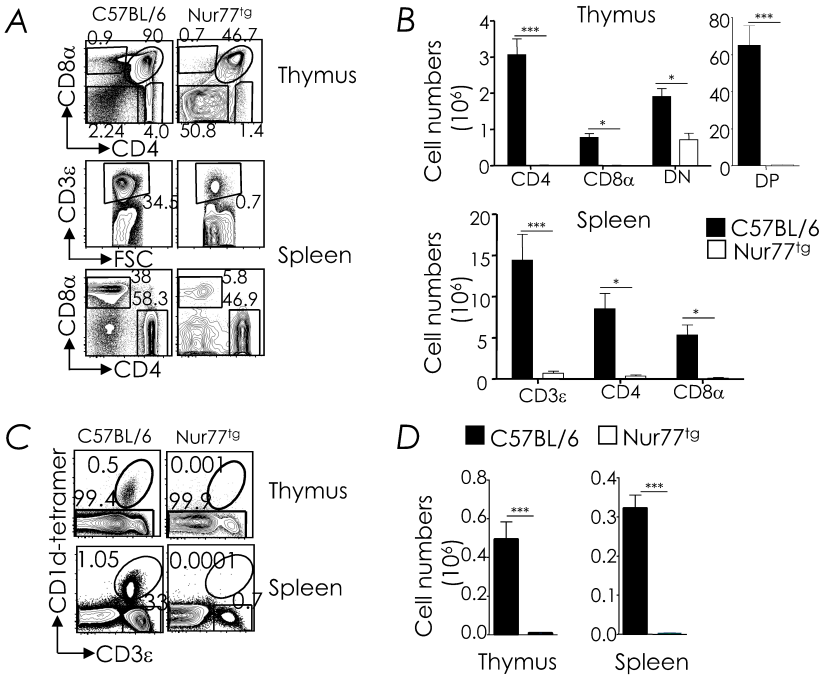

Figure S1. Constitutive overexpression of Nur77 impairs conventional T cell development. (**A**) Thymic and splenic $CD4^+$ and $CD8^+$ T cells from C57BL/6 (*n*=5) and $Nur77^{tg}$ (*n*=4) mice were identified within electronically gated $CD3\varepsilon^+tetramer^{NEG}$ thymocytes or $B220^{NEG}CD3\varepsilon^+$ splenocytes. Numbers are % $CD4^+$ or $CD8^+$ T cells among total leukocytes. Data are representative of two independent experiments. (**B**) Absolute cell numbers were calculated by multiplying total cell counts with the frequency (%) of $CD4^+$, $CD8^+$, $CD4^+8^+$ DP or $CD4^{NEG}8^{NEG}$ DN cells. *n*, as in **A**. Data are cumulative mean ± sem (standard error of the mean) from two independent experiments. (**C**) Thymic and splenic iNKT cells from C57BL/6 (*n*=4) and $Nur77^{tg}$ (*n*=4) mice were identified as $CD3\varepsilon^+tetramer^+$ cells within electronically gated $CD8^{lo}$ thymocytes or $B220^{lo}$ splenocytes. Numbers are % iNKT cells among total leukocytes within each organ. (**D**) Absolute cell numbers were calculated by multiplying total cell counts with the frequency (%) of % iNKT cells. Data are cumulative mean ± sem; *n*, as in **C**. $*P \leq 0.05$, $***P \leq 0.0001$.

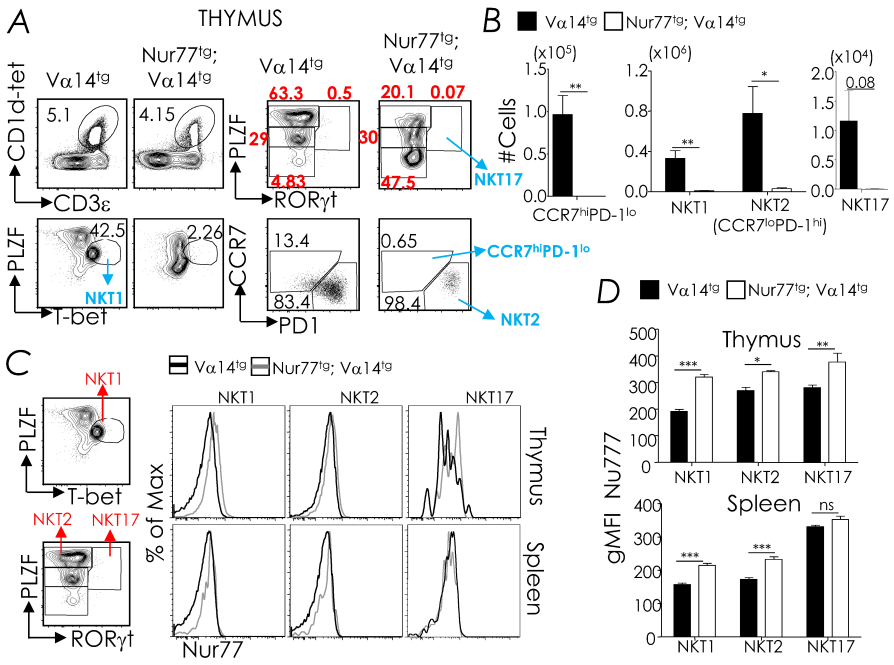

Figure S2. Introgression of a rearranged *Vα14i* TCR α-chain gene into Nur77^{tg} mice partially rescues iNKT cell development. (**A**) iNKT cells in thymus from Nur77^{tg};Vα14^{tg} (*n*=3) and Vα14^{tg} (*n*=3) mice were identified as in **Fig. S1**, and surface stained with mAbs against mouse CCR7 and PD-1. Then they were stained with specific mAb for PLZF, T-bet and RORγt. Contour plots show gating strategy to identify PLZ^{HI}, PLZF^{INT} and PLZF^{LO} (all RORγt^{NEG}) and PLZF^{HI}RORγt^{+} NKT17 iNKT cells. PLZF^{HI} population were further gated to identify CCR7^{HI}PD-1^{LO} and CCR7^{LO}PD-1^{HI} (NKT2) cells. PLZF^{INT}Tbet^{HI} NKT1 cells were identified by gating for T-bet expression on iNKT cells. Plots are representative of two independent experiments. (**B**) Absolute numbers of iNKT subsets were calculated by multiplying the frequency (%) of iNKT cells with total cell number. Data are cumulative mean ± sem from two independent experiments. *n*, as in **A**. (**C,D**) iNKT cells identified as above from the thymus and spleen of Nur77^{tg};Vα14^{tg} (*n*=3) and Vα14^{tg} (*n*=3) mice were segregated into iNKT subsets, PLZF^{INT}Tbet^{HI} NKT1, PLZF^{HI} NKT2, PLZF^{HI}RORγt^{+} NKT17 cells (**C**; contour plots, left panel), and Nur77 expression monitored. (**C**) Overlay histograms are representative of two independent experiments. (**D**) gMFI of Nur77 expression by thymic (top panel) and splenic (bottom panel) iNKT cell subsets. Data are cumulative mean ± sem; *n*, as in **C.** ns, not significant ($P > 0.05$), *$P \leq 0.05$, **$P \leq 0.001$, ***$P \leq 0.0001$.

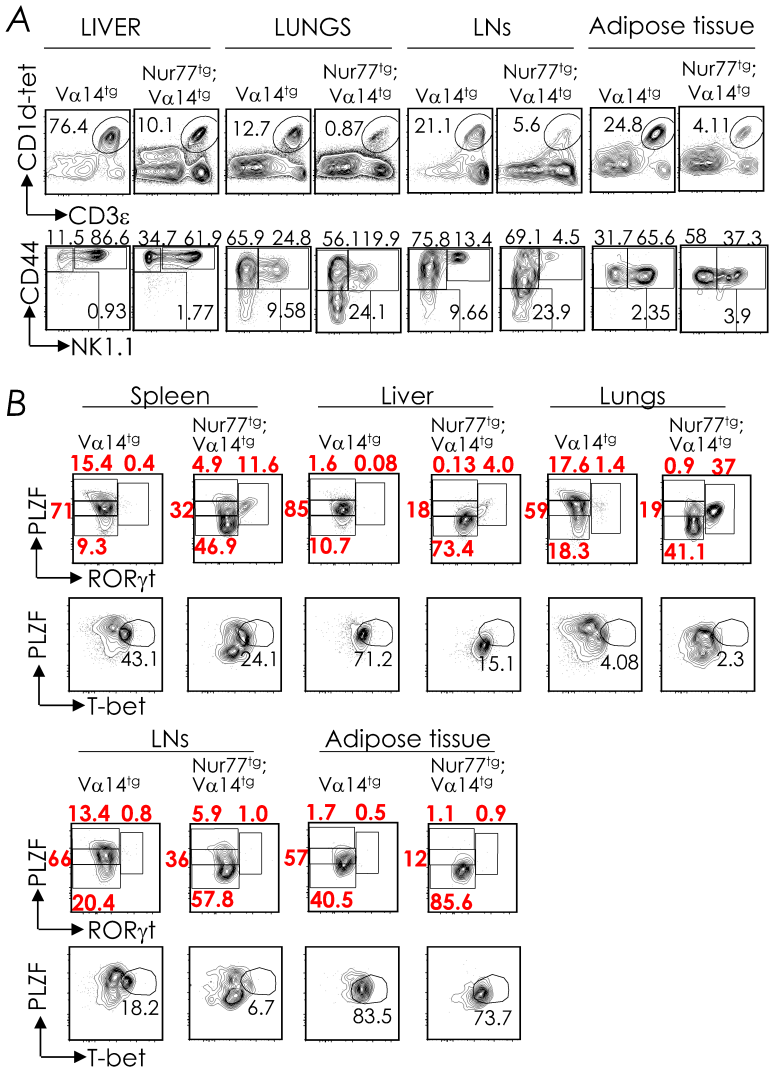

Figure S3. Nur77 overexpression alters peripheral iNKT cells in Nur77^{tg};Vα14^{tg} mice. (**A**) iNKT cells (upper panels) in indicated organs from Nur77^{tg};Vα14^{tg} (*n*=3) and Vα14^{tg} (*n*=3) mice were identified as in **Fig. 1A**. iNKT cell stages (lower panels) were identified as in **Fig. 1C**. Contour plots are representative of two independent experiments. (**B**) iNKT cell subsets were identified in spleen, liver, lungs, lymph nodes and adipose tissue from Nur77^{tg};Vα14^{tg} (*n*=3) and Vα14^{tg} (*n*=3) mice as in **Fig S2C**. Contour plots are representative of two independent experiments.

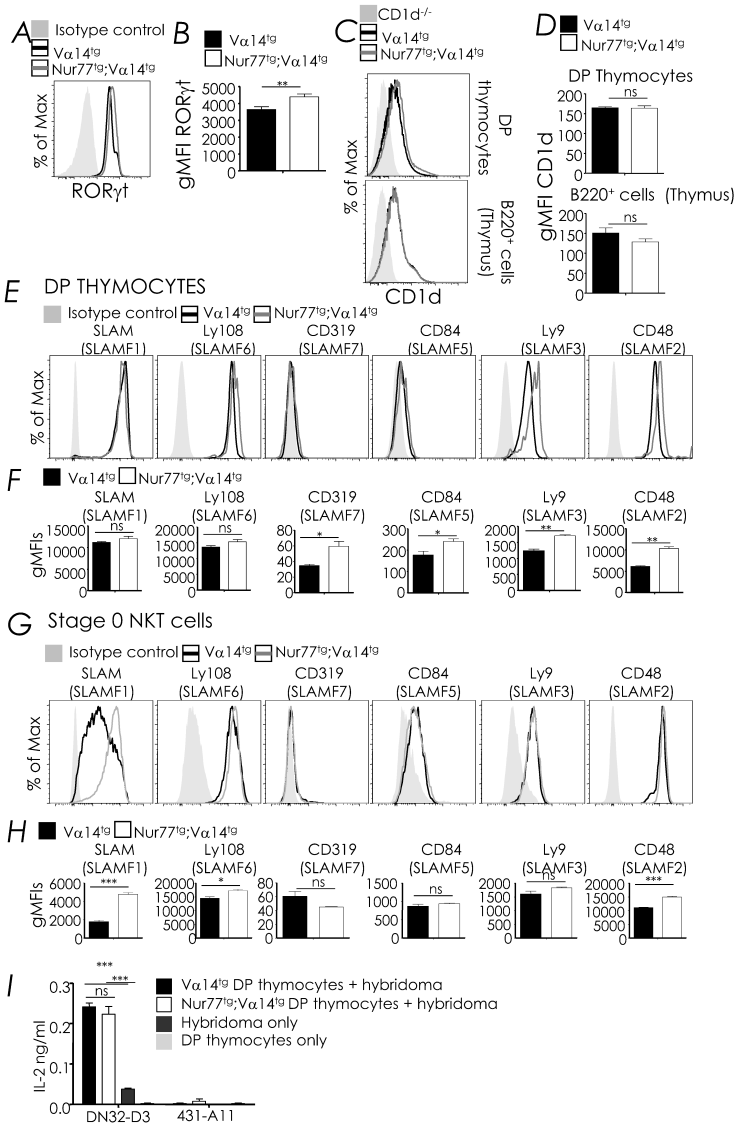

Figure S4. Normal CD1d, SLAM receptors, and endogenous agonistic ligand expression. (**A,B**) RORγt levels in DP thymocytes from Vα14^{tg} (*n*=9), Nur77^{tg}Vα14^{tg} (*n*=6) mice are shown; overlay histograms (**A**) and gMFIs indicative of RORγt level (**B**) are shown. Data are cumulative mean ± sem from three independent experiments. (**C,D**) Thymic DP T cells and B220^{+} cells from Vα14^{tg} (*n*=4), Nur77^{tg}Vα14^{tg} (*n*=3) mice were identified within electronically gated CD3ε^{+} tetramer^{NEG} thymocytes and monitored for CD1d expression. CD1d$^{-/-}$ mice were used as control. (**C**) Overlay histograms are representative of three independent experiments. (**D**) gMFI of CD1d expression on DP thymocytes and B220^{+} cells from thymus are shown. Data are cumulative mean ± sem; *n*, as in **C**. (**E—H**) Expression of SLAM receptors: SLAM (SLAMF1; CD150), Ly108 (SLAMF6; NTB-A), CD319 (SLAMF7; CRACC), CD84 (SLAMF5), Ly9 (SLAMF3; CD229), CD48 (SLAMF2) by DP T cells (**E,F**) and stage 0 iNKT cells (**G,H**) identified as above were tracked on Vα14^{tg} (*n*=3), Nur77^{tg}Vα14^{tg} (*n*=4) mice. Overlay histograms (**E,G**) and gMFIs (**F,H**) are shown. Data are cumulative mean ± sem from two independent experiments. (**I**) IL-2 production by a Vα14^{+} iNKT cell hybridoma DN32.D3 and control Vα3.2^{+} hybridoma 431-A11 co-cultivated with the indicated flow sorted DP thymocytes at 10:1 DP thymocytes:hybridoma ration or alone. Data are cumulative mean ± sem from two independent experiments. ns, not significant (P >0.05), *P ≤ 0.05, **P ≤0.001, ***P≤0.0001.

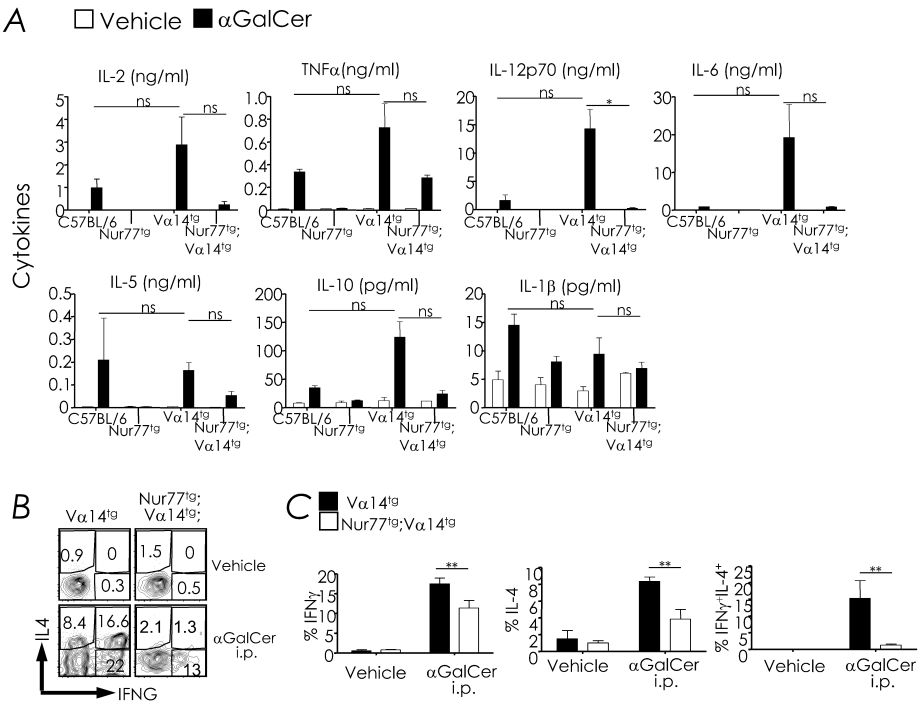

Figure S5. iNKT cells in Nur77^{tg};Vα14^{tg} mice recognize αGalCer but are hyporesponsive. (**A**) αGalCer or vehicle control was injected i.p. into B6, Nur77^{tg}, Nur77^{tg};Vα14^{tg} and Vα14^{tg} mice. Six hours post injection, serum was harvested, and cytokines measured using meso scale detection kit. Data are cumulative mean ± sem from two independent experiments; B6 (vehicle *n*=2; αGC *n*=2), Nur77^{tg} (vehicle *n*=2; αGC *n*=2), Nur77^{tg};Vα14^{tg} (vehicle *n*=2; αGC *n*=4) and Vα14^{tg} (vehicle *n*=2; αGC *n*=3). (**B,C**) Splenic iNKT cells from Vα14^{tg} and Nur77^{tg};Vα14^{tg} mice injected i.p. with vehicle control or 1 μg αGalCer were evaluated for intracellular IFN-γ and IL-4 expression 6 hours post injection. Contour plots are representative of 3—4 independent experiments. Vα14^{tg} (vehicle *n*=4; αGC *n*=4), Nur77^{tg};Vα14^{tg} (vehicle *n*=4; αGC *n*=4) (**B**) and % IFN-γ^{+}, % IL-4^{+}, and % IFN-γ^{+}IL-4^{+} iNKT cells (**C**) are shown. Data are mean ± sem. ns, not significant ($P > 0.05$), *$P \leq 0.05$, **$P \leq 0.001$.

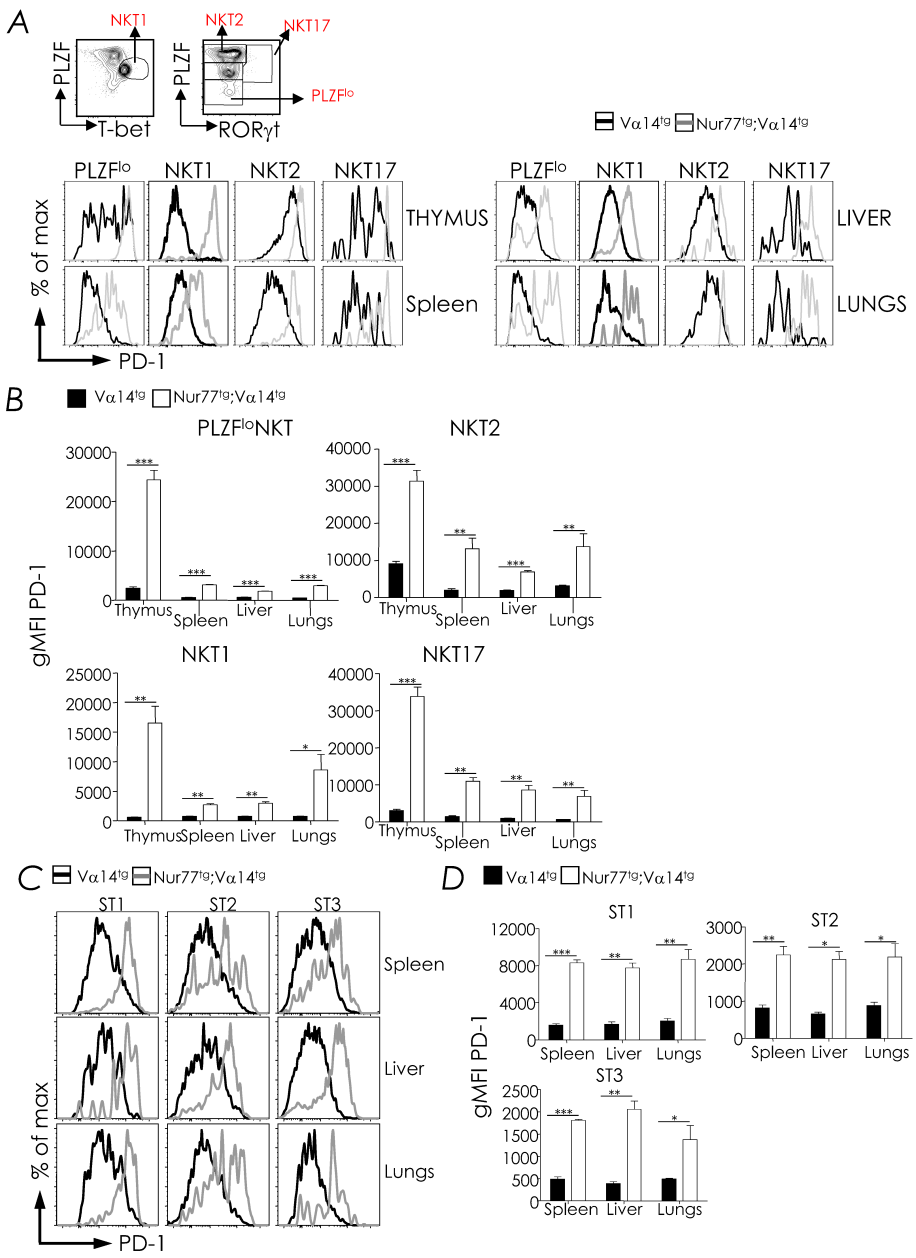

Figure S6. iNKT cells in Nur77^{tg};Vα14^{tg} mice have exhausted phenotype. (**A,B**) iNKT cells in Vα14^{tg} (*n*=3) and Nur77^{tg};Vα14^{tg} (*n*=3) mice were surface stained with mAbs against mouse PD-1. Then they were stained with specific mAb for PLZF, T-bet and RORγt. Contour plots showing gating strategy to identify PLZF^{LO}, PLZF^{INT}Tbet^{HI} NKT1, PLZF^{HI} NKT2, PLZF^{HI}RORγt^{+} NKT17 iNKT cells. PD-1 expression was monitored on the indicated iNKT cell populations. (**A**) Overlay histograms are representative of two independent experiments. (**B**) gMFIs of PD1 expression. Data are cumulative mean ± sem from two independent experiments. (**C**—D) iNKT cell developmental stages were identified as CD44^{NEG}NK1.1^{NEG} stage 1, CD44^{+}NK1.1^{NEG} stage 2, or CD44^{+}NK1.1^{+} stage 3 in spleen, liver and lungs. (**C**) Overlay histograms are representative of two independent experiments, *n* as in **A.** (**D**) gMFIs of PD1 expression. Data are mean ± sem from two independent experiments, *n* as in A **P* ≤ 0.05, ***P* ≤0.001. ****P* ≤0.0001.

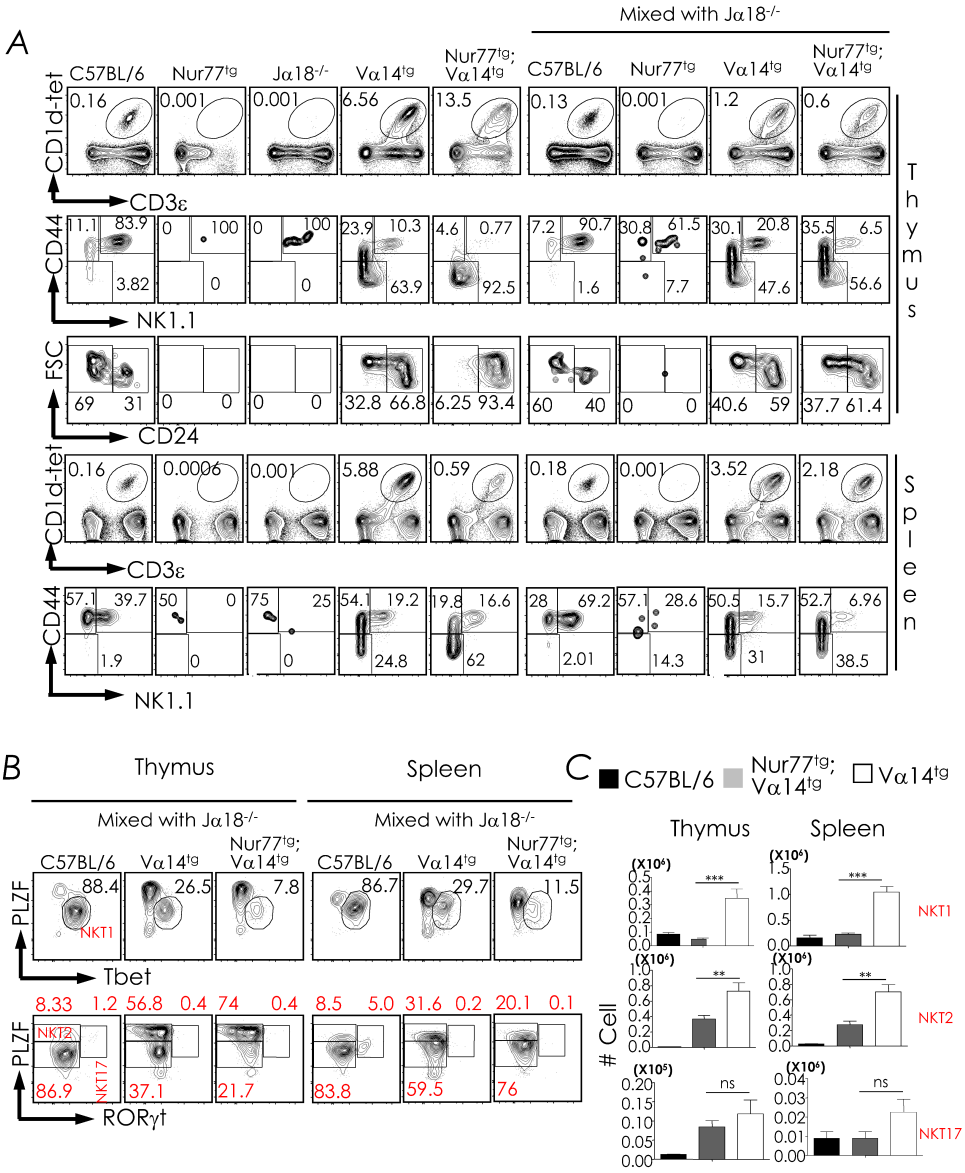

Figure S7. Impaired iNKT cell development in Nur77^{tg};Vα14^{tg}/Jα18$^{-/-}$ mice owes to cell-intrinsic and cell-extrinsic defects. (A) Analysis of chimeras generated with BM cells from donor B6, Nur77^{tg}, Jα18$^{-/-}$, Nur77^{tg};Vα14^{tg} or Vα14^{tg} mice transferred into irradiated Jα18$^{-/-}$ recipients alone (single BM chimeras) or mixed with BM from Jα18$^{-/-}$ at 1:1 ratio (mixed BM chimeras). Thymic and splenic iNKT cells from B6 (*n*=6), Nur77^{tg} (*n*=6), Jα18$^{-/-}$ (*n*=4), Nur77^{tg};Vα14^{tg} (*n*=6), Vα14^{tg} (*n*=6) single BM chimeras and B6 (*n*=5), Nur77^{tg} (*n*=5), Nur77^{tg};Vα14^{tg} (*n*=25), Vα14^{tg} (*n*=20) mixed BM chimeras were identified as before (rows 1 and 4, respectively). iNKT cell developmental stages were identified as stage 0+1, stage 2, and stage 3 in the thymus and spleen (rows 2 and 5, respectively). In the thymus, stage 0+1 cells were further gated to distinguish stage 0 from stage 1 iNKT cells (row 3). Numbers are % cells among total iNKT cells. (B,C)Thymocytes and splenocytes from B6 (*n*=4), Nur77^{tg};Vα14^{tg} (n=18), and Vα14^{tg} (*n*=14) mixed BM chimeras were surface stained to identify iNKT cells, followed by nuclear staining with specific mAb against PLZF, T-bet and RORγt. (B) iNKT cell subsets were identified as PLZF^{INT}T-bet^{HI} NKT1 (upper panel), PLZF^{HI} NKT2, and PLZF^{HI}RORγt^{+} NKT17 (lower panel) subsets in the thymus and spleen. Numbers are % cells among total iNKT cells. Contour plots are representative of 3—5 independent experiments. (C) Absolute numbers of NKT1, NKT2 or NKT17 cells were calculated multiplying the absolute iNKT cell number with the frequency (%) of NKT1, NKT2 or NKT17 cells in B. Data are mean ± sem from three or more independent experiments. *n*, as in B. not significant ($P > 0.05$), ** $P \leq 0.001$, *** $P \leq 0.0001$.

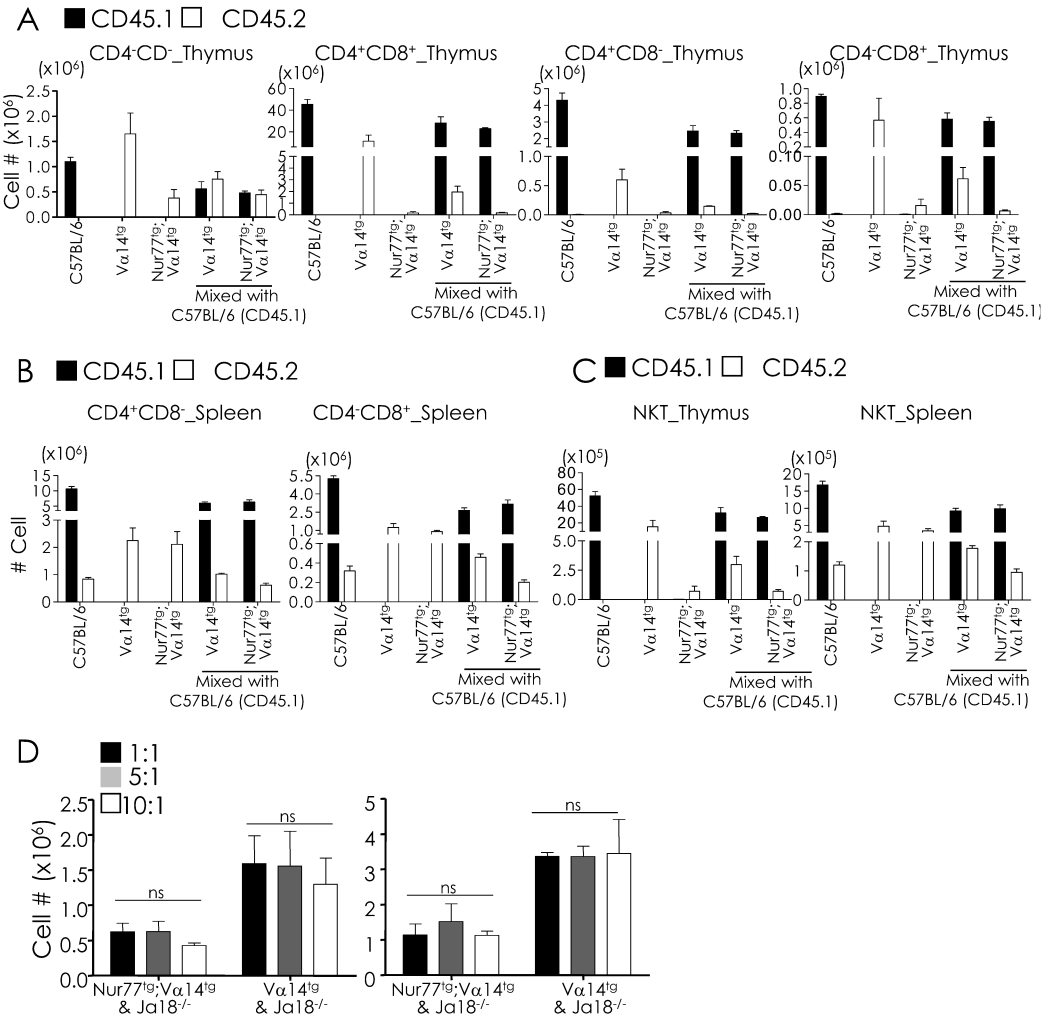

Figure S8. Impaired iNKT cell development in Nur77^{tg};Vα14^{tg}/Jα18$^{-/-}$ mice owes to cell-intrinsic and cell-extrinsic defects. (**A—C**) BM cells from donor CD45.1$^+$ B6 (*n*=3), CD45.2$^+$ Vα14^{tg} (*n*=2) or CD45.2$^+$ Nur77^{tg};Vα14^{tg} (*n*=2) mice were transferred into irradiated Jα18$^{-/-}$ recipients alone (single BM chimeras) or BM cells from CD45.1$^+$ B6 mice were mixed at 1:1 ratio with BM cells from CD45.2$^+$ Vα14^{tg} (*n*=4) or CD45.2$^+$ Nur77^{tg};Vα14^{tg} (*n*=5) mice to generate mixed BM chimeras. (**A,B**) Thymic CD4$^+$, CD8$^+$, DP, DN T cells and splenic CD4$^+$ and CD8$^+$ T cells were identified as in **Fig. S1A**. Bar graphs show total T cell numbers, which was calculated as in **Fig. 1B**, in CD45.1$^+$ and CD45.2$^+$ gated thymocytes (**A**) and splenocytes (**B**). Data are mean±sem from 2 experiments. *n* as in **A**. (**C**) Thymic and splenic iNKT cells were identified as before in single and mixed BM chimeras. Bar graphs showing absolute iNKT cell numbers in thymus and spleen gated for CD45.1 and CD45.2 expression. Data are mean ± sem from two experiments. *n* as in **A**. (**D**) BM cells (1x10^6, 5x10^6 or 10x10^6) from Jα18$^{-/-}$ mice were mixed with 10x10^6 BM cells from Vα14^{tg} or Nur77^{tg};Vα14^{tg} BM cells, yielding 10:1, 5:1, 1:1 ratio of BM cells from the two strains. These were mixed and transferred into irradiated Jα18$^{-/-}$ recipients. iNKT cells were identified as in **Fig. S1C**. Bar graphs show absolute iNKT cell number calculated as in **Fig. 1D**. Data are mean ± sem from two experiments (Vα14^{tg}/Jα18$^{-/-}$ mixed BM chimeras *n*=4 for each ratio tested; Nur77^{tg};Vα14^{tg}/Jα18$^{-/-}$ mixed BM chimeras *n*=6, 4 and 4, respectively, for 1:1, 5:1 and 10:1 ratio). ns, not significant, $P>0.05$, $^{**}P\leq0.001$, $^{***}P\leq0.0001$.

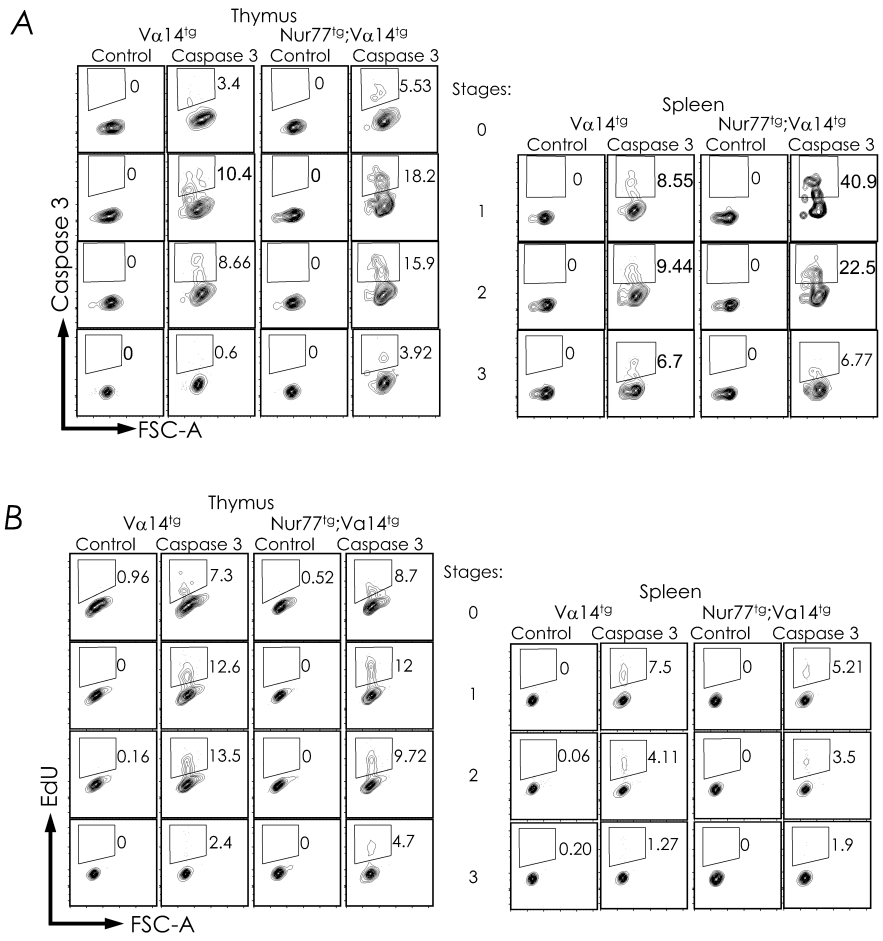

Figure S9. Enhanced iNKT cell apoptosis in Nur77^{tg};Vα14^{tg}/Jα18$^{-/-}$ mixed BM chimeras. (**A**) Thymocytes and splenocytes from Vα14^{tg}/Jα18$^{-/-}$ (*n*=5) single and Nur77^{tg};Vα14^{tg}/Jα18$^{-/-}$ (*n*=5) mixed BM chimeras were treated with fluorescently-tagged, active caspase or control substrates. After four hours, iNKT cells and iNKT cell developmental stages were identified and caspase-3 incorporation monitored. (**A**) Contour plots are representative of two independent experiments. (**B**) Vα14^{tg}/Jα18$^{-/-}$ (*n*=3) and Nur77^{tg};Vα14^{tg}/Jα18$^{-/-}$ (*n*=3) mixed BM chimeras were injected i.p. with 1 mg EdU or PBS control. About 72 hours later, thymocytes and splenocytes were stained for EdU incorporation at various iNKT cell developmental stages. Contour plots are representative of two independent experiments.

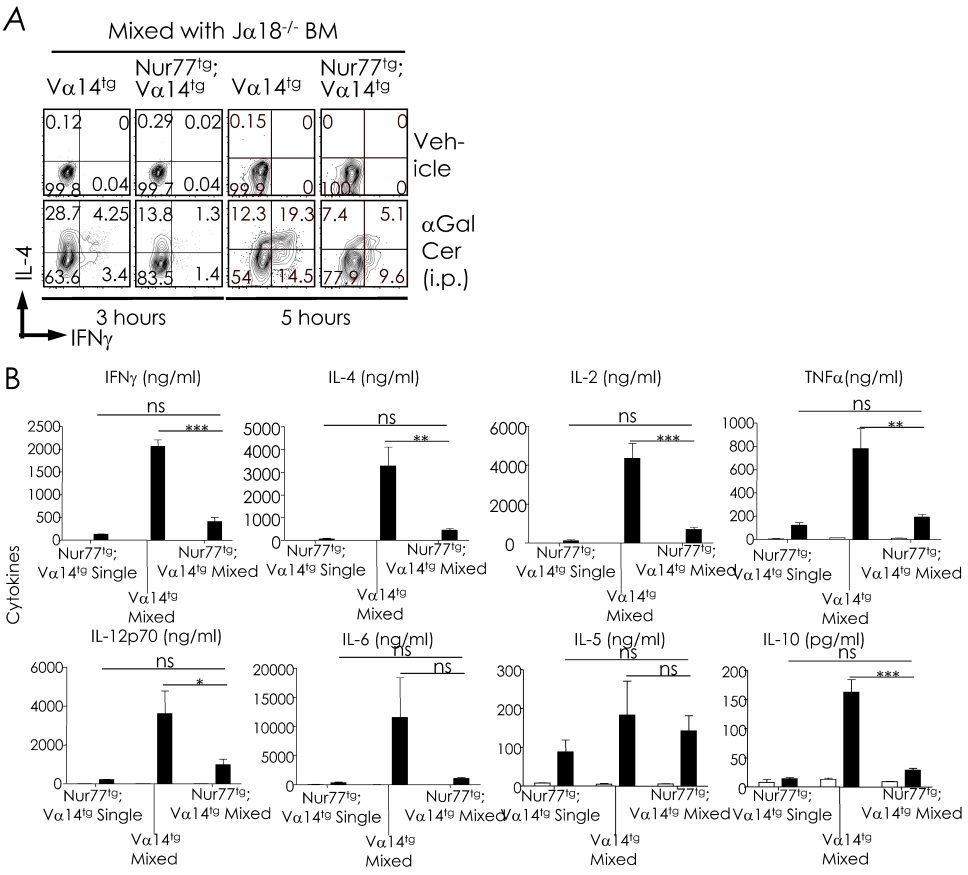

Figure S10. iNKT cells in Nur77^{tg};Vα14^{tg}/Jα18$^{-/-}$ mixed BM chimeras respond poorly to in vivo αGalCer stimulation. (A) Vα14^{tg}/Jα18$^{-/-}$ and Nur77^{tg};Vα14^{tg}/Jα18$^{-/-}$ mixed BM chimeras were injected i.p. with vehicle or 1 μg αGC. Spleens were harvested at the indicated times after injection. Splenocytes were surface stained to identify iNKT cells and stained with mAb to detect intracellular IFN-γ and IL-4. Dot plots showing IFN-γ^{+} and IL-4^{+} iNKT cells. Data are representative of 3—5 independent experiments. *n* for 3 hours: Vα14^{tg}/Jα18$^{-/-}$ (Veh=3, αGC=3), Nur77^{tg};Vα14^{tg}/Jα18$^{-/-}$ (Veh=5, αGC=7); *n* for 5 hours; Vα14^{tg}/Jα18$^{-/-}$ (Veh=5, αGC=6), Nur77^{tg};Vα14^{tg}/Jα18$^{-/-}$ (Veh=7, αGC=9). (**B**) Single Nur77^{tg} BM chimeras or mixed Vα14^{tg}/Jα18$^{-/-}$ or Nur77^{tg};Vα14^{tg}/Jα18$^{-/-}$ BM chimeras were injected with vehicle or 1 μg αGalCer i.p. followed by serum harvest after 6 hours. Serum cytokine levels were determined by meso scale detection multiplex cytokine assay. Data are mean ± sem. *n* for Nur77^{tg} single chimera: Veh=2, αGC=3; Vα14^{tg}/Jα18$^{-/-}$ mixed chimera: Veh=3, αGC=3; and Nur77^{tg};Vα14^{tg}/Jα18$^{-/-}$ mixed chimera: Veh=4, αGC=5. ns, not significant ($P > 0.05$), *$P \leq 0.05$, **$P \leq 0.001$, ***$P \leq 0.0001$.

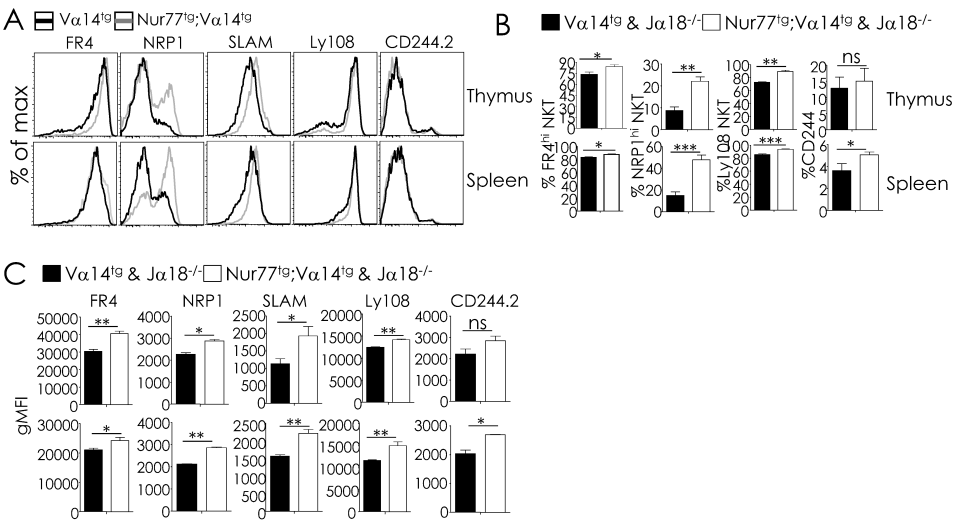

Figure S11. iNKT cells in Nur77^{tg};Vα14^{tg}/Jα18$^{-/-}$ mixed BM chimeras express Treg/NKT10 markers (**A—C**) Surface expression of FR4, NRP, SLAM, Ly108 and CD244.2 on thymic and splenic iNKT cells identified as **in Fig. 1C** was evaluated in Vα14^{tg}/Jα18$^{-/-}$ (*n*=4) and Nur77^{tg};Vα14^{tg}/Jα18$^{-/-}$ (*n*=6) mixed BM chimeras. (**A**) Overlays are representative of two independent experiments. *n* as above. (**B**) Bar graphs show % of iNKT cells expressing FR4^{HI}, NRP1^{HI}, Ly108^{HI}, and CD244.2^{HI} iNKT cells in Vα14^{tg}/Jα18$^{-/-}$ and Nur77^{tg};Vα14^{tg}/Jα18$^{-/-}$ mixed BM chimeras. Data are mean ± sem. *n* as in **A**. (**C**) gMFI of FR4, NRP1, SLAM, Ly108 and CD244.2 on thymic and splenic iNKT cells in mixed BM chimeras. Data are mean ± sem. *n* as in **A**. ns $P > 0.05$, * $P \leq 0.05$, ** $P \leq 0.001$, *** $P \leq 0.0001$.

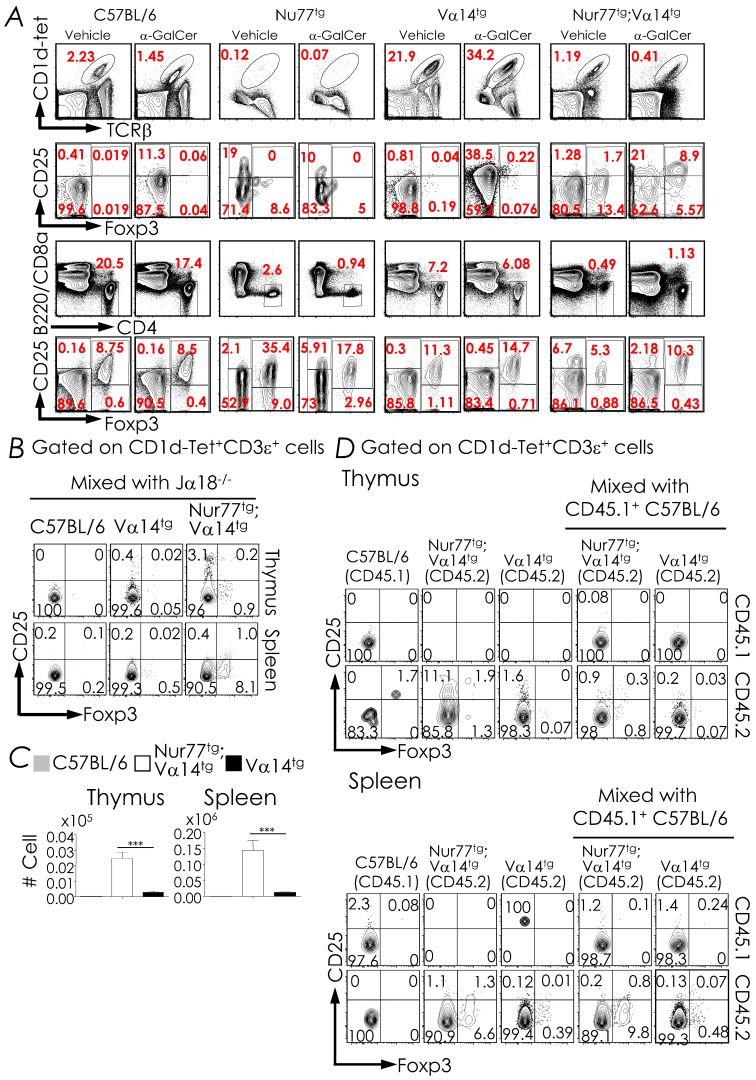

Figure S12. Nur77 induces Foxp3$^+$ iNKT cells in Nur77^{tg};Vα14^{tg}/Jα18$^{-/-}$ mixed chimeras. (A) Splenocytes from C57BL/6, Nur77^{tg}, Vα14^{tg}, and Nur77^{tg};Vα14^{tg} mice injected with vehicle or αGalCer were stained to identify iNKT cells and CD4$^+$ T cells as in **Fig. S1**, and CD25 and Foxp3 expression on iNKT cells and CD4$^+$ T cells were monitored. Representative contour plots from three independent experiments show CD25 and Foxp3 expression by iNKT cells (upper two rows) and CD4$^+$ T cells (lower two rows). *n*= C57BL/6 (Veh=5, αGC=5), Nur77^{tg} (Veh=3, αGC=4), Vα14^{tg} (Veh=4, αGC=4) and Nur77^{tg};Vα14^{tg} (Veh=4, αGC=5). (**B,C**) Thymic and splenic iNKT cells in B6/Jα18$^{-/-}$ (*n*=2), Vα14^{tg}/Jα18$^{-/-}$ (*n*=7), and Nur77^{tg};Vα14^{tg}/Jα18$^{-/-}$ (*n*=7) mixed BM chimeras generated as in **Fig. S4** were identified as in **Fig. S1C**, and surface CD25 and nuclear Foxp3 expression evaluated. (**B**) Contour plots are representative of three independent experiments. *n* as above. (**C**) Bar graphs show cumulative mean ± sem of % of CD25^{NEG}Foxp3$^+$ iNKT cells. *n* as in **A**. (**D**) BM cells from congenically marked donor CD45.1$^+$ C57BL/6 (*n*=3), CD45.2$^+$ Vα14^{tg} (*n*=2) or CD45.2$^+$ Nur77^{tg};Vα14^{tg} (*n*=2) mice were transferred into irradiated Jα18$^{-/-}$ recipients either alone (single chimeras), or mixed at 1:1 ratio with BM cells from CD45.2$^+$ Vα14^{tg} (*n*=4) or CD45.2$^+$ Nur77^{tg};Vα14^{tg} (*n*=5) mice to generate mixed BM chimeras. Thymic and splenic iNKT cells were identified as in **Fig. S1C**, and surface CD25 and nuclear Foxp3 expression evaluated. Contour plots are representative of two independent experiments. ***$P \leq 0.0001$.

Table S1. List of antibodies used for multiparametric iNKT cells analyses in this study

Antigen	Fluorochrome*	Clone	Source**
CD1d-αGalCer tetramer	APC, BV421	Mouse CD1d	in-house [1]; NIH Tetrmer Core (Emory University)
CD3ε	PE, PerCP-Cy5.5, APC, PE-Cy7	145-2C11	BD Biosciences, BioLegend, Tonbo Biosciences
CD8α	FITC, PerCP-Cy5.5, APC-Cy7	53-6.7	BD Biosciences, BioLegend, eBiosciences
TCRβ	BV421, APC-eF780	H57-597	Biolegend, BD Biosceinces
CD44	FITC, APC-Cy7	IM7	BD Biosciences
NK1.1	PE, PerCP-Cy5.5, APC, APC-Cy7	PK136	BD Biosciences
B220	FITC, PerCP-Cy5.5, APC-Cy7	RA3-6B2	BD Biosciences
CD4	FITC, PE, PerCP-Cy5.5	RM4-4	BD Biosciences, BioLegend
CD69	FITC, PE, PE-Cy7, APC	H1.2F3	BD Biosciences
CD122	FITC	TM-b1	Biolegend
CD24	FITC	M1/69	BD Biosciences
CD25	PE-Cy7	PC61	BD Biosciences
PLZF	PE	9E12	Biolegend
Nur77	PE	12.14	eBiosciences
T-bet	APC	4B10	BioLegend
RORγt	PerCP-Cy5.5	Q31-378	BD Biosciences
Foxp3	PE, APC	FJK-16s	eBiosciences
PD-1	PE, PE-Cy7, APC	1A12	BioLegend
CCR7	BV605	4B12	BioLegend
Cd1d	PE	1B1	BD Biosciences
SLAM (SLAMF1)	BV-421	TCF15-12F12.2	BioLegend

Antigen	Fluorochrome*	Clone	Source**
Ly108 (SLAMF6)	PE	330-AJ	BioLegend
CD319 (SLAMF7)	APC	$G2	BioLegend
CD84 (SLAMF5)	PE	mCD84.7	BioLegend
Ly9 (SLAMF3)	PE	Ly9ab3	BioLegend
CD48 (SLAMF2)	APC	HM48-1	BioLegend
IFN-γ	FITC, APC	XMG1.2	BioLegend
IL-4	PE	11B11	BioLegend
IL-10	PE	JESS-16E3	BioLegend
IL-17	PE	TC11-188H10.1	BioLegend
FR-4	PE	12A5	BioLegend
NRP-1	BV421	3E12	BioLegend
CD244.2	APC	eBio244F4	eBiosciences

*APC, allophycocyannin; Cy, cyanine; PE, phycoerythrin; PerCP, peridinin chlorophyll protein; APC-Cy7, tandem allophycocyannin-cyanine 7 dye

**where multiple sources are indicated, the reagent worked equally well from the different sources

SI LITERATURE CITED

1. Kumar A, Bezbradica JS, Stanic AK, Joyce S. Characterization and Functional Analysis of Mouse Semi-invariant Natural T Cells. *Current Protocols in Immunology* **117**, 14.13.11-14.13.55 (2017); doi: 10.1002/cpim.22

2. Kumar A*, et al.* NF-kappaB Protects NKT Cells from Tumor Necrosis Factor Receptor 1-induced Death. *Scientific Reports* **7**, 15594 (2017); doi: 10.1038/s41598-017-15461-y